LAUTECH Journal of Engineering and Technology 20 (1) 2026: 13-27
10.36108/laujet/6202.02.0120

Green Synthesis and Characterization of Tin (IV) Oxide Nanoparticles from Fresh and Dried *Senna alata* Leaf Extract

[1]Adegboyega O., [2]Ojo O. P., [3]Olabisi O., [4]Alamu G. A. and [4]Adedokun O.

[1]Department of Physics, Emmanuel Alayande University of Education, Oyo, Nigeria
[2]Department of Biology, Emmanuel Alayande University of Education, Oyo, Nigeria
[3]Department of Science Laboratory Technology, Ladoke Akintola University of Technology, Ogbomoso, Nigeria
[4]Department of Pure and Applied Physics, Ladoke Akintola University of Technology, Ogbomoso, Nigeria

Article Info

Article history:

Received: Nov 30, 2025
Revised: Dec 11, 2025
Accepted: Dec 29, 2025

Keywords:

Biosynthesis, SnO_2 Nanoparticles, *Senna alata*, Structural properties, Optical properties, Thermal conductivities

Corresponding Author:
oadedokun@lautech.edu.ng

ABSTRACT

Despite the growing interest in plant-mediated nanoparticle synthesis, limited research has examined how the condition of plant material (fresh or dried) has affected the efficiency and quality of synthesized nanoparticles. This study reports the green synthesis of tin (IV) oxide (SnO_2) nanoparticles using aqueous extracts from fresh and dried Senna alata leaf as reducing, stabilizing, and capping agents, with 1.0 M Tin (II) chloride dihydrate ($SnCl_2{\cdot}2H_2O$) as the precursor. Structural, morphological, optical, and thermal properties of the synthesized nanoparticles were investigated. XRD analysis confirmed the formation of crystalline tetragonal rutile-phase SnO_2, with average crystallite sizes of 3.7 nm for fresh-leaf extract and 8.19 nm for dried-leaf extract. FTIR spectra revealed stronger and more distinct functional groups (O–H, C–H, C–O, and NO_3^-) in nanoparticles derived from fresh extracts. SEM and TEM analyses showed uniformly distributed, spherical nanoparticles with minimal agglomeration and average particle sizes of 9.88 nm (fresh extract) and 9.80 nm (dried extract). EDX analysis confirmed elemental purity with dominant Sn and O signals and complete removal of chlorine residues. Optical studies demonstrated that fresh-leaf-derived nanoparticles exhibited higher absorbance, lower transmittance, and a narrower band gap (3.21 eV) compared to the dried-leaf counterpart (3.58 eV). Thermal conductivity results indicated superior heat-transport performance for nanoparticles synthesized from fresh leaves, particularly at lower temperatures. These findings demonstrated that fresh Senna alata leaf extract provides a potential sustainable and efficient route for producing high-quality SnO_2 nanoparticles with enhanced optical and thermal properties for advanced technological applications.

INTRODUCTION

Nanotechnology is projected to constitute a major part of the next technological revolution, which is the fourth generation of industrialization to occur in this modern era; Industry 4.0. Hence, the production and analysis of nanoparticles, which are the fundamental component of nanotechnology, and their properties has become one of the most active subjects of significant research in modern material sciences.

SnO_2 has been prepared using various syntheses that can be broadly categorized into conventional and green methods. Conventional approaches include solid-state synthesis, hydrothermal methods (Narasaiah *et al*., 2022), sol-gel method (Karmaoui *et al.,* 2018), colloidal and aerosol routes, chemical vapor deposition, and co-precipitation techniques.

In recent years, green synthesis methods have emerged as attractive to traditional chemical and physical synthesis methods (Abiodun *et al*., 2024a).

The green synthetic approach using plant extracts attracted the researchers due to their simplicity and ecofriendly approach (Lithi *et al.,* 2025 & Villagran *et al.,* 2024). It is cost effective and therefore can be used as an economic and viable alternative for the large-scale production of metal oxide nanoparticles (Lithi *et al.,* 2025). The rate of nano synthesis or the stability of the product depends on the reducing agents and capping agents used during the synthesis of nanomaterials. In the green synthesis of nanomaterials, the alkaloids, flavones, terpenes, amino acids and carbohydrates present in the plant materials act as the reducing agents and capping agents which plays a major role on the surface morphology and size of the metals (Singh *et al*., 2023). Plant materials offer a free source of pigments, such as carotene and chlorophyll, which acts act as sensitizers (Adedokun *et al*., 2018). Abiodun *et al*., (2024a) stressed the importance of incorporation of green-synthesized copper oxide nanoparticles into the counter electrode of Monolithic Dye-Sensitized Solar Cells (MDSSC) as eco-benign and even dispersion, suggested its potential as promising nanomaterial for DSSC application. Abiodun *et al*., (2024b) stated that the potential of incorporating green-synthesized iron oxide nanoparticles into MDSSC counter electrodes was shown by their great biocompatibility and even dispersion.

Metal oxide nanoparticles show a great demand in the chemical, electronic and pharmaceutical industries (Narayanan, 2012; Hariprasad *et al.,* 2016). Among the nano metal oxides, SnO_2 NPs have been studied intensively because of their potential applicability to lithium-ion batteries, transparent conducting electrodes in ionic devices, anti-reflective coatings, solid-state gas sensors, solar cells, catalytic support materials, energy storage, medicals, etc. (Buniyamin et al., 2023).

In spite of extensive reports on plant-assisted nanoparticle synthesis, critical synthesis parameters remain insufficiently understood, particularly the physiological condition of the plant material used. One such parameter (the use of fresh versus dried leaves) has been shown to influence nanoparticle formation. Aondona *et al.* (2018) reported that dried leaf extracts were more efficient than fresh leaf extracts in the biosynthesis of silver nanoparticles, attributing this improvement to increased phytochemical concentration and stability following drying. However, these findings are largely confined to noble metal nanoparticles and may not directly translate to metal oxide systems, where nanoparticle formation involves additional processes such as hydrolysis, oxidation, and defect formation. Recent studies have shown that plant extracts significantly influence the crystallinity, particle size, and optical properties of metal oxide nanoparticles, including SnO_2, with solvent and extract composition playing key roles (Sivarajan *et al.*, 2025; Matussin *et al*., 2020). Consequently, the influence of leaf physiological condition on the synthesis of metal oxide nanoparticles particularly SnO_2 remains underexplored and poorly understood.

Tin (II) chloride dihydrate ($SnCl_2{\cdot}2H_2O$) is widely employed as a precursor for SnO_2 synthesis owing to its high solubility, ease of hydrolysis, and suitability for low-temperature green synthesis routes (Matussin *et al*., 2020). Its interaction with plant-derived phytochemicals enables efficient conversion to SnO_2 nanoparticles under mild reaction conditions. *Senna alata* was selected as the biological reagent in this study due to its rich phytochemical composition, wide availability, non-toxicity, and reported antioxidant activity (Sarwar *et al*., 2025).

In this present study, extracts of fresh leaves of *Senna alata* and its dried version were used to establish the comparative efficacy of the fresh leaves with respect to the dried version in the biosynthesis of SnO_2 NPs while water was used as

solvent medium. The objective of this work is to establish the comparative efficacy of the abovementioned fresh leaves with respect to dried leaves extract in the biosynthesis of SnO_2 NPs. The synthesized nanoparticles were thoroughly characterized using techniques such as X-ray Diffraction (XRD), Fourier Transform Infrared Spectroscopy (FTIR), Energy dispersive X-ray Spectroscopy (EDX), Scanning electrons Microscopy (SEM), Transmission electrons microscopy (TEM), UV-Visible spectroscopy and Thermal conductivity analyzer, to confirm their structural, morphological optical and thermal properties, respectively.

METHODOLOGY

Materials

The leaf of *Senna alata* (candlestick plant) was acquired from a farm in the Baale Yaku area, located at 8.14319^0 North and 4.19674^0 East in Ogbomoso, Oyo State, Nigeria. Distilled water was used as extraction solvent. Analytical-grade of $SnCl_2{\cdot}2H_2O$ was purchased from a local supplier and used without further purification.

Methods

Preparation of *Senna alata* Leaf Extracts

Senna alata leaf was collected and prepared according to established protocols for phytochemical extraction. Fresh leaves were initially rinsed thoroughly with clean water to eliminate dust and surface impurities. For phytochemical extraction, distilled water was selected as the extraction solvent due to its high efficiency in dissolving bioactive compounds and its recognition as a safe, effective, and environmentally friendly option for plant-based extractions (Karmaoui *et al*., 2018).

Fresh *senna alata* leaves of 1.0 g and 100 ml of distilled were finely grounded for 10 min using an electric blender, and the resulting mixture was filtered through Whatman No. 1 filter paper. The crude fresh leaf extract (FSAW) obtained exhibited an amber-brown coloration and was stored in a beaker for subsequent use.

For the preparation of extracts from dried leaves, a slightly modified procedure was employed. Fresh leaves were initially rinsed with clean water and subsequently air-dried under shade at ambient room temperature (25–30°C) for 10 days. This shade-drying method was specifically chosen to preserve key phytochemicals such as anthraquinones, flavonoids, carotenoids, and phenolic compounds (Yagi *et al*., 2024), as these compounds are known to degrade when exposed to direct sunlight or elevated temperatures. Following the same extraction procedure as the fresh leaves, distilled water was used as the extraction solvent. The dried leaves were grounded using an electric blender, and the resulting extracts were filtered through Whatman No. 1 filter paper, yielding a reddish-brown coloured crude dried leaf extract (DSAW) that was stored in a beaker for further analysis.

Synthesis of SnO_2 Nanoparticles

Tin oxide nanoparticles were synthesized using a simple precipitation method with plant extract mediation. A 1.0 M solution of $SnCl_2{\cdot}2H_2O$ was prepared by dissolving the salt in 100 mL of distilled water in a separate beaker. The solution was stirred for 120 seconds using a magnetic stirrer, resulting in a milky white suspension.

In the typical synthesis procedure, the aqueous Senna alata leaf extract was added dropwise to the $SnCl_2{\cdot}2H_2O$ solution at a volume ratio of 1:10, following established green synthesis protocols (Rahim *et al*., 2022). The phytochemicals present in the plant extract served as natural reducing and stabilizing agents, facilitating the

reduction of Sn^{2+} ions to SnO_2 nanoparticles (Villagran *at a*l., 2024). Distinct colour changes were observed immediately, indicating the formation of nanoparticles. A mixture of the aqueous fresh Senna alata leaf extract and $SnCl_2.2H_2O$ solution (FSAW+$SnCl_2$ Solution) change to lemon-yellow colour while a mixture of the aqueous dried Senna alata leaf extract and $SnCl_2.2H_2O$ solution (DSAW+$SnCl_2$ Solution) change to orange-yellow colour. This colour change is characteristic of SnO_2 nanoparticle formation and can be used as a preliminary indicator of synthesis success (Narasaiah *et al*., 2022).

The resulting mixture was centrifuged at 4000rpm for 10 min using a Model 800 centrifuge, and the supernatant was decanted to separate the solid particles. The pellets were then carefully removed and dried in an oven at 60°C for 24 hours to obtain the final SnO_2 nanoparticle product. This drying temperature was selected to prevent thermal degradation of any residual organic capping agents derived from the plant extract while ensuring complete removal of moisture (Rahim *et al*., 2022). All samples were properly labeled and stored at ambient room temperature (25–30 °C) until further C) until further use.

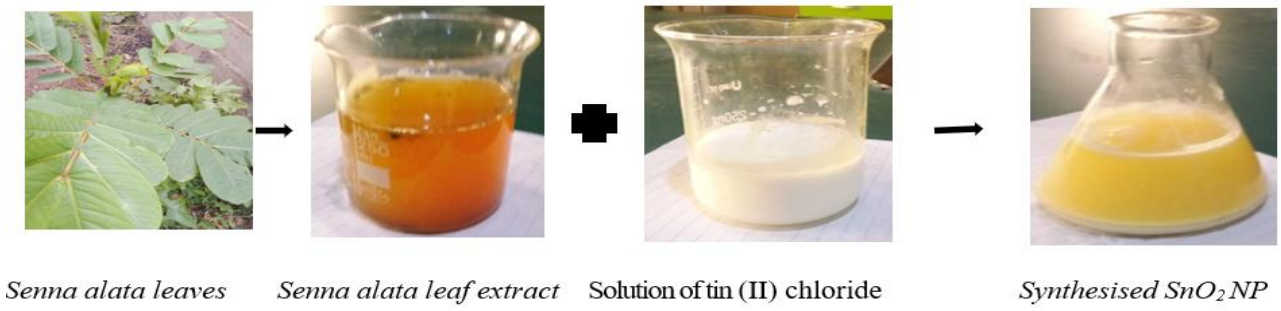

Plate 1: Synthesis of SnO_2 NP using a mixture of the aqueous fresh *Senna alata* leaf extract and $SnCl_2.2H_2O$ solution .

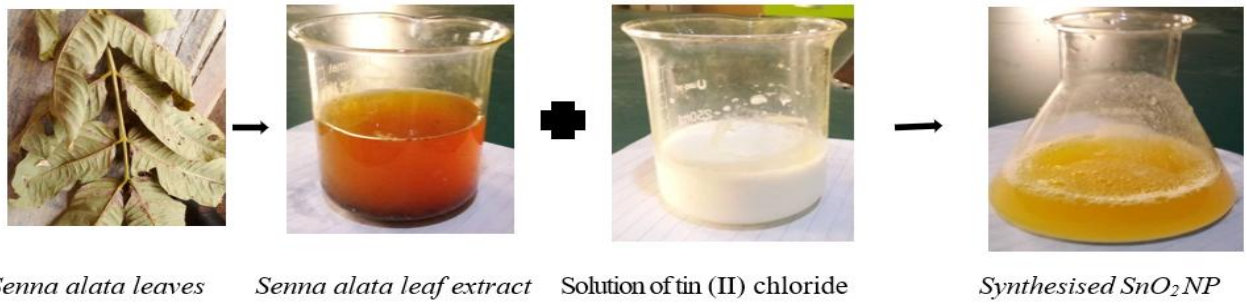

Plate 2: Synthesis of SnO_2 NP using a mixture of the aqueous dried s*enna alata* leaf extract and $SnCl_2.2H_2O$ solution

Characterization of SnO_2 Nanoparticles

The characterization of nanoparticles is important for understanding their properties and applications. The crystallographic structure and phase composition of the synthesized SnO_2 nanoparticles were analyzed using X-ray diffraction (XRD) on a Rigaku diffractometer, following general XRD data acquisition and interpretation practices outlined in ASTM E975. Functional groups and chemical bonding characteristics were examined using Fourier Transform Infrared (FTIR) spectroscopy with an Agilent Cary 630, and spectra were interpreted in accordance with ASTM E1252 guidelines for qualitative infrared analysis. The surface morphology and elemental composition of the nanoparticles were investigated by Scanning

Electron Microscopy (SEM) coupled with Energy Dispersive X-ray (EDX) spectroscopy (JEOL JBM-7600F), with elemental analysis conducted following ASTM E1508 recommendations. High-resolution Transmission Electron Microscopy (TEM) analysis was performed using a Verios 460L to evaluate particle size, morphology, and lattice structure, in alignment with general electron microscopy practices described in ASTM E986. The optical properties of the SnO_2 nanoparticles were characterized using UV–Visible spectroscopy on a JASCO V-670 over the wavelength range of 200–900 nm, and the optical bandgap energy was estimated from the absorption spectra using Tauc plot analysis in accordance with ASTM E903. Thermal conductivity measurements were carried out using a 212R Trace Thermal Conductivity Analyzer under steady-state conditions, following the principles outlined in ASTM D5470 for evaluating the thermal transmission properties of thermally conductive materials.

RESULTS AND DISCUSSION

Structural characterization of the Synthesized SnO_2 Nanoparticles

XRD characterization of the synthesized SnO_2 Nanoparticles

The XRD patterns of SnO_2 nanoparticles prepared are presented in Figure 1. The major diffraction peaks are labelled (002), (101), (200) and (220), which correspond well to the tetragonal rutile phase of SnO_2 (JCPDS) card no. 41-1445). The results are consonant with the submission of Alanazi *et al*. (2023) and Letifi *et al.* (2021). The presence of sharp peaks, especially (002), indicates a crystalline structure (Letifi *et al*., 2021). No significant impurity peaks were observed, suggesting the success of pure SnO_2, as similarly reported for biosynthesis methods (Buniyamin et al., 2023). The Structural parameters were shown in table 1. The average crystallite size ($\boldsymbol{L_a}$, $\boldsymbol{L_b}$,), Full Width at Half Maximum ($\boldsymbol{\beta_a}$, $\boldsymbol{\beta_b}$,) and d spacing ($\boldsymbol{d_a}$, $\boldsymbol{d_b}$,) were also presented in table 2. Comparatively, the aqueous fresh *Senna alata* leaf extract with the tin (II) chloride dihydrate solution (FSAW + $SnCl_2$ solution), favoured smaller particles, possibly due to faster reaction kinetics and greater phytochemical activity (Yagi et al., 2024). The higher concentration of bioactive compounds in fresh plant material, particularly flavonoids and phenolic compounds, likely accelerated the nucleation and growth processes during nanoparticle formation (Karmaoui et al., 2018), resulting in improved size control and crystallinity.

FTIR Characterization of the Synthesized SnO_2 Nanoparticles

FTIR measurements were probed to assess the influence of a change in the condition of leaf extraction on the structural properties of the synthesized SnO_2 nanoparticles, and the results are shown in Figure 2. As seen in Table 3, the absorbance peak of C-O stretching mode is situated at 1050.00 cm^{-1} in FSAW+$SnCl_2$ and 1038.00 cm^{-1} in DSAW+$SnCl_2$. Besides, the FTIR bands at 1622.00 cm^{-1} signifying $\boldsymbol{NO_3^-}$ stretching mode in FSAW+$SnCl_2$ and 1595.00cm^{-1} in DSAW+$SnCl_2$. The absorption band at 3482.00 cm^{-1} in FSAW+$SnCl_2$ signifying the presence of OH stretching vibration of surface hydroxyl group or adsorbed water, and the peak at 2926.00 cm^{-1} in (a) confirms the presence of C-H vibration or stretching mode (Toloman *et al*., 2014; *Blessi et al*., 2014), which have already reduced in size in DSAW+$SnCl_2$ 3392.00 cm^{-1} and 2918 cm^{-1} respectively. This is largely due to the change in the condition of the Senna alata leaf, i.e. from fresh to dry.

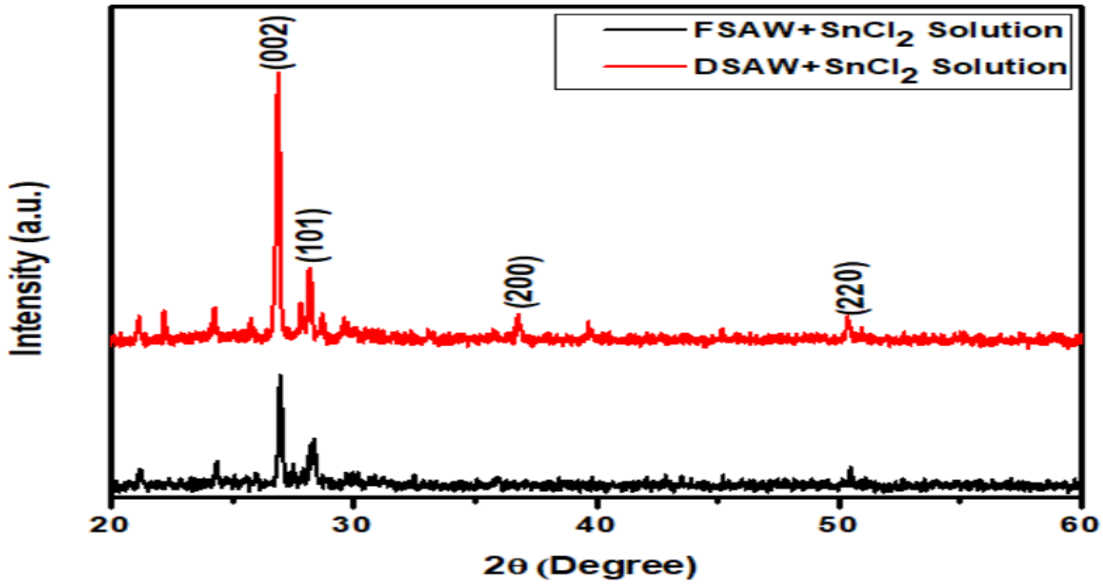

Figure 1: XRD patterns of synthesized SnO_2 nanoparticles extracted FSAW+$SnCl_2$ and DSAW+$SnCl_2$

Table 1: Structural parameter of SnO_2 Nanoparticles: FSAW + $SnCl_2$ and DSAW + $SnCl_2$

2θ (°)		L (nm)		β (°)		d (nm) × 10^{-1}	
$2\theta_a$	$2\theta_b$	L_a	L_b	β_a	β_b	d_a	d_b
27.0	27.0	3.63	7.99	2.35	1.06	3.3	3.3
28.0	28.2	3.64	8.02	2.35	1.06	3.1	3.2
36.1	36.2	3.66	8.06	2.35	1.06	2.9	2.0
50.2	50.4	3.90	8.69	2.35	1.06	`1.8	1.8

Table 2: The average crystallite size, Full Width at Half Maximum and d spacing of Synthesized SnO_2

Sample	Leaf Type	Solvent	Crystalline Size (nm)	FWHM (°)	d-Spacing (nm)
FSAW + $SnCl_2$	Fresh	Water	3.70	2.35	0.2775
DSAW + $SnCl_2$	Dry	Water	8.19	1.06	0.2575

Table 3: Summary of bond types and wavenumber in synthesized SnO_2 Nanoparticles: FSAW + $SnCl_2$ and DSAW + $SnCl_2$

Peak	Wave number (cm^{-1})		Bond type
	FSAW+$SnCl_2$	DSAW+$SnCl_2$	
1	3482.00	3392.00	OH stretch
2	2926.00	2918.00	C-H stretch
3	1622.00	1595.00	NO_3^- stretch
4	1050.00	1038.00	C-O stretch

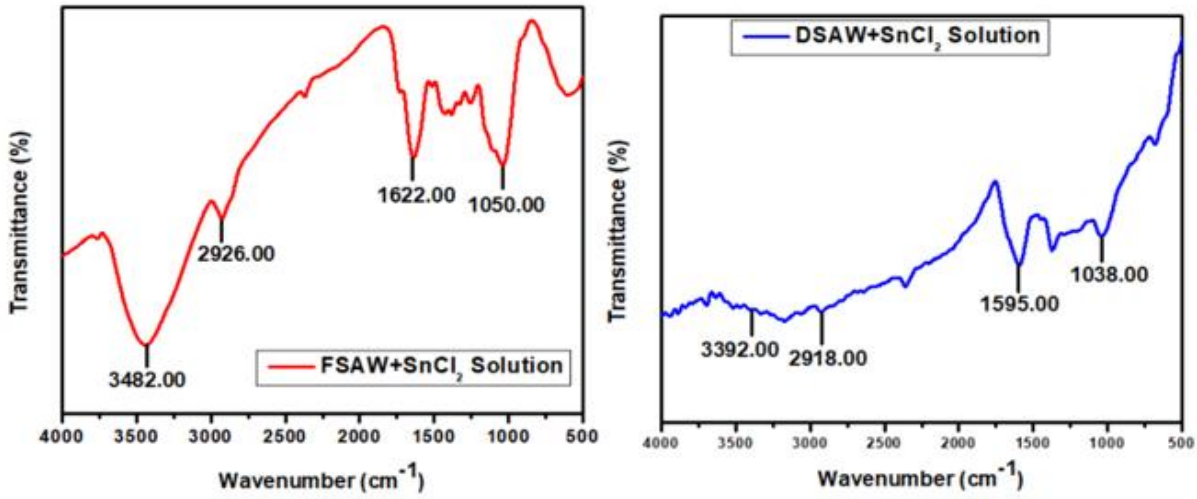

Figure 2: FTIR spectra of synthesized SnO_2 nanoparticles extracted FSAW+$SnCl_2$ and DSAW+$SnCl_2$

Morphological Properties of the Synthesized SnO_2 Nanoparticles

SEM Characterization of the Synthesized SnO_2 Nanoparticles

Figure 3 shows the SEM images of synthesized SnO_2 nanoparticles. The SEM images demonstrate high film coverage and uniform morphology. The images show the presence of homogeneous and well-dispersed spherical nanoparticles, as also reported by Alanazi *et al.* (2023), and some of them are partially aggregated in the form of irregularly shaped nanoparticles typical of SnO_2. Individual SnO_2 crystallites were apparent and well-defined. There is evidence of rounding at the edges of the crystallites, and a measure of disfigurement was observed in FSAW+$SnCl_2$, indicating low-level adherence and crystallinity of SnO_2 nanoparticles formed (Saravanakumar *et al*., 2014). It was observed that synthesized SnO_2 nanoparticles extracted in FSAW+$SnCl_2$ showed improved surface morphology compared to those extracted in DSAW+$SnCl_2$.

TEM Characterization of the synthesized SnO_2 Nanoparticles

Figure 4 shows the TEM micrographs of synthesized SnO_2 nanoparticles. The TEM micrographs in FSAW+$SnCl_2$ and DSAW+$SnCl_2$ revealed the presence of non-agglomerated SnO_2 nanoparticles (NPs) with uniform particle size and average sizes of 9.88 nm (fresh extract) and 9.80 nm (dried extract). No coalescence or aggregation of the nanoparticles was observed, demonstrating that the organic ligands at the nanoparticle surface could produce adequate steric force to enable well-separated nanoparticles. This finding agrees with reports denoting that biosynthesis produces stable, well-dispersed nanoparticles due to natural capping agents present in plant extracts (Buniyamin *et al*., 2023).

EDX Characterization of the synthesized SnO_2 Nanoparticles

The energy dispersive spectra of synthesized SnO_2 nanoparticles are shown in in Figure 5. The illustration of the tin oxide nanoparticle spectrum was composed of tin (Sn), oxygen (O), carbon (C), silicon (Si), iron (Fe), Sulphur (S), potassium (K), calcium (Ca), copper (Cu), sodium (Na), magnesium (Mg) and excludes of chlorine (Cl) ions. This confirmed that the SnO_2 nanoparticles were free from Cl ions. And again, the synthesized SnO_2 nanoparticles spectra predominantly consist of tin (Sn) and oxygen (O) while carbon (C), silicon (Si), iron (Fe), Sulphur (S), potassium (K), calcium (Ca),

copper (Cu), sodium (Na), magnesium (Mg) present essentially in small quantities. As seen in Figure 5, FSAW+$SnCl_2$ showed the percentage compositions of 40.0% and 20.5% for Sn and O, respectively; DSAW+$SnCl_2$ showed 45.0% and 10.1% for Sn and O, respectively. Impurities such as carbon (C), silicon (Si), iron (Fe), Sulphur (S), potassium (K), calcium (Ca), copper (Cu), sodium (Na), magnesium (Mg) were also manifested in the synthesized SnO_2 nanoparticles, probably owing to the plant residue, and the instrument used. The EDX confirmed purity and the absence of chlorine residues. These elemental composition findings are consistent with EDX analyses reported in the literature for biogenically synthesized SnO_2 nanoparticles, where trace elements from plant sources are commonly observed as surface modifications (Alzahrani *et al*., 2023).

Optical characterization of the Synthesized SnO_2 Nanoparticles

Absorbance–Wavelength Plots

Figure 6(a) shows the UV–visible absorbance spectra of $SnCl_2$ solution, aqueous fresh (FSAW*)* and dried (*DSAW*) *Senna alata* leaf extracts, and their respective mixtures with $SnCl_2$. The pure $SnCl_2$ solution exhibited a relatively low average absorbance of 0.38 with a sharp peak around 280 nm, corresponding to charge transfer transitions of ionic Sn^{2+} species. The FSAW and DSAW extracts showed higher average absorbance values of 0.52 and 0.47, respectively, with peaks near 270–275 nm. These bands are attributed to $\pi\rightarrow\pi^*$ and $n\rightarrow\pi^*$ transitions of phenolic and flavonoid compounds, confirming the presence of chromophoric biomolecules capable of reducing and stabilising metal ions.

Upon mixing with $SnCl_2$, the absorbance increased significantly, reaching 0.96 for FSAW + $SnCl_2$ and 0.79 for DSAW + $SnCl_2$, with new, broader bands extending between 300 and 450 nm, which could be attributed to the intrinsic band gap absorption of SnO_2 (Letifi *et al*., 2021). The higher absorbance of the FSAW + $SnCl_2$ mixture shows that the fresh extract possessed stronger reducing and capping ability than the dried extract, leading to greater particle density and enhanced optical activity, consistent with established findings on plant-mediated nanoparticle synthesis (Haq *et al*., 2022).

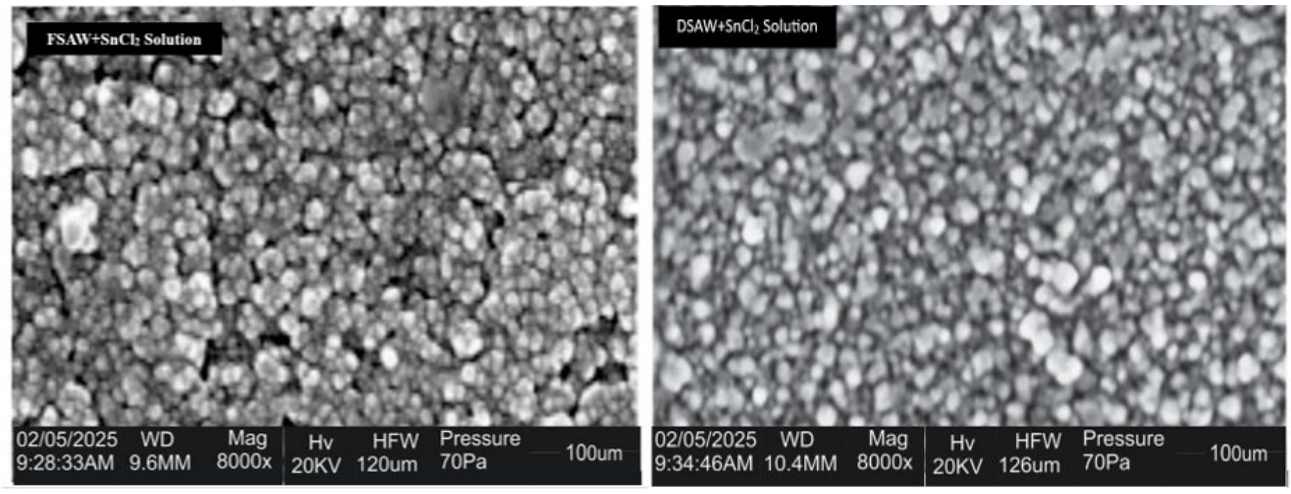

Figure 3: SEM images of synthesized SnO_2 nanoparticles extracted FSAW+$SnCl_2$, and DSAW+$SnCl_2$

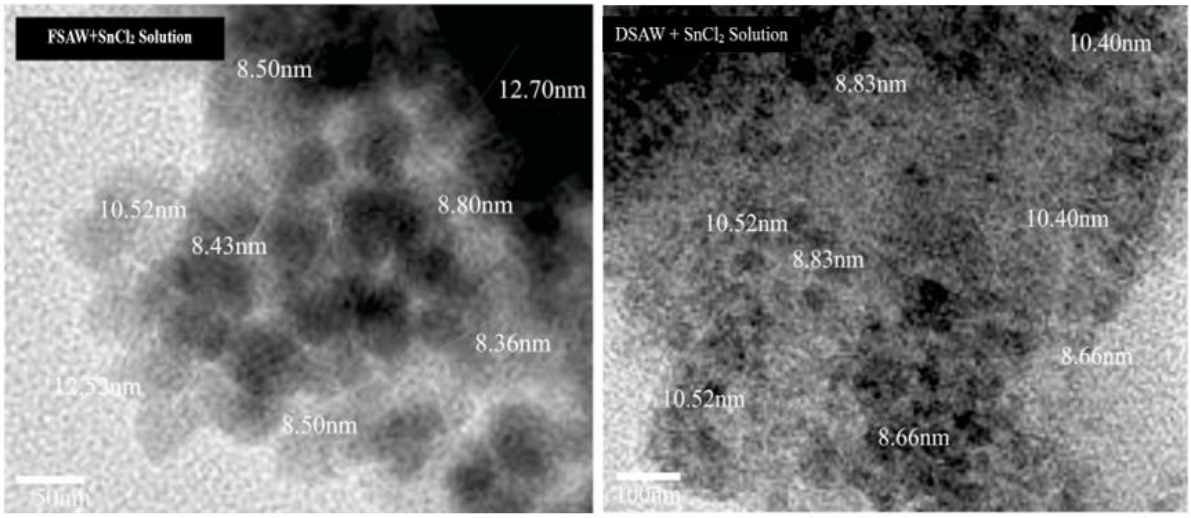

Figure 4: TEM images of synthesized SnO_2 nanoparticles extracted FSAW+$SnCl_2$ and DSAW+$SnCl_2$

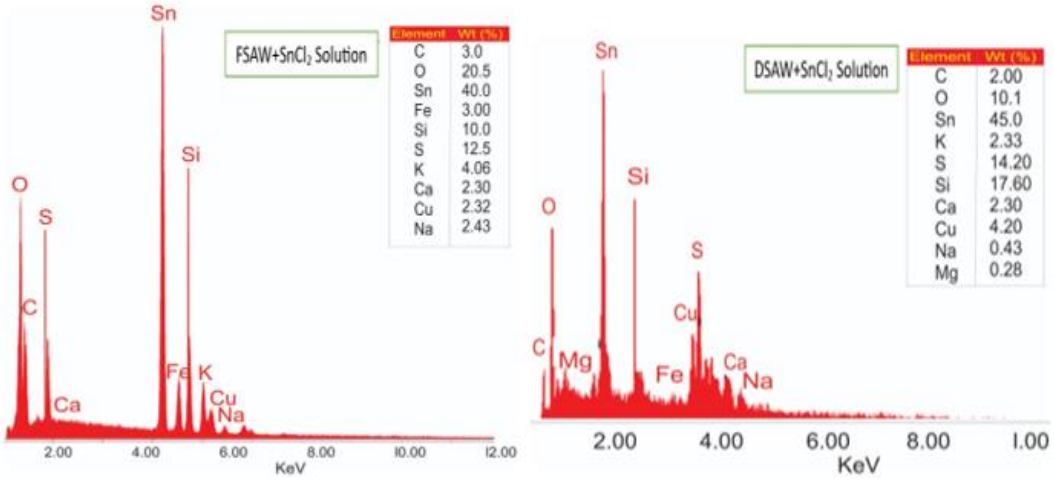

Figure 5: EDX Spectra of synthesized SnO_2 nanoparticles extracted FSAW+$SnCl_2$ and DSAW+$SnCl_2$

The high absorbance values, especially for the FSAW + $SnCl_2$ sample, confirm efficient light harvesting and nanoparticle formation. These optical properties make the biosynthesized SnO_2 nanoparticles potential for photocatalytic degradation**,** UV-shielding coatings**,** solar energy devices**,** and gas-sensing applications, where strong UV absorption enhances performance.

Transmittance–Wavelength Plots

The transmittance spectra Figure 6(b) complement the absorbance data. The $SnCl_2$ solution exhibited the highest average transmittance of 68.4%**,** consistent with its low absorbance and transparency. FSAW and DSAW had moderate transmittance values of 60.2% and 63.1%**,** respectively, reflecting the presence of light-absorbing phytochemicals. When mixed with $SnCl_2$, transmittance dropped sharply to 39.8% for FSAW + $SnCl_2$ and 47.6% for DSAW + $SnCl_2$, particularly below 400 nm. This reduction confirms that the mixtures absorb and scatter more light due to the formation of SnO_2 nanoparticles.

The inverse relationship between absorbance and transmittance shows that nanoparticle growth significantly affects optical transparency. The FSAW + $SnCl_2$ sample, exhibiting the lowest transmittance (39.8%), suggests the presence of a denser particle suspension (Haq *et al*., 2022). Such

optical attenuation properties are beneficial for UV-filtering materials, transparent conductive oxides, and photoactive films, where controlled light transmission is desirable.

Tauc Plot and Optical Band Gap

Figure 7(a) displays the Tauc plots used to determine the optical band gap (Eg) of the samples. Also, Figure 7(b) shows the variation of optical band gap (Eg) of the samples. The measured Eg values were 3.81 eV ($SnCl_2$), 4.28 eV (FSAW), 4.34 eV (DSAW), 3.21 eV (FSAW + $SnCl_2$), and 3.58 eV (DSAW + $SnCl_2$). The band gap energies of theses NPs displayed direct electronic transitions (Chen *et al*., 2017, Kaur *et al*., 2023; Chaitra *et al.*, 2023). The reduction in Eg upon combining $SnCl_2$ with the extracts confirms the transformation from ionic tin species to semiconducting SnO_2 nanoparticles. The lowest Eg (3.21 eV) observed for the FSAW + $SnCl_2$ system indicates a higher degree of electronic delocalization and enhanced formation of smaller, well-dispersed nanoparticles. The band gap values obtained are consistent with published values for biogenically synthesized SnO_2 nanoparticles, which typically range from 3.0 to 3.7 eV depending on particle size, synthesis methodology, and any doping elements (Din *et al*., 2022).

The narrowed band gaps improve photon absorption and charge transfer efficiency, making the biosynthesized SnO_2 nanoparticles promising for photocatalysis, solar energy harvesting, UV photodetectors, and gas sensors. The demonstrated ability to tailor Eg through selection of plant extract type and optimization of synthesis route enables precise control of optical and electronic properties for targeted end-use applications (Letifi *et al*., 2021).

Collectively, the optical spectra confirm that *Senna alata* leaf extracts, particularly the fresh extract can act as both reducing and capping agents in the green synthesis of SnO_2 nanoparticles. The optical characteristics (strong UV absorption, reduced transmittance, and narrowed band gap) demonstrate that these biosynthesized nanoparticles possess desirable semiconducting and photoactive properties, potential for sustainable applications in environmental remediation, energy harvesting, and sensing technologies.

Thermal Conductivity of the Synthesized SnO_2 Nanoparticles

Table 4 presents the thermal conductivity values of synthesized SnO_2 nanoparticles measured at six different temperatures ranging from 50°C to 300°C.

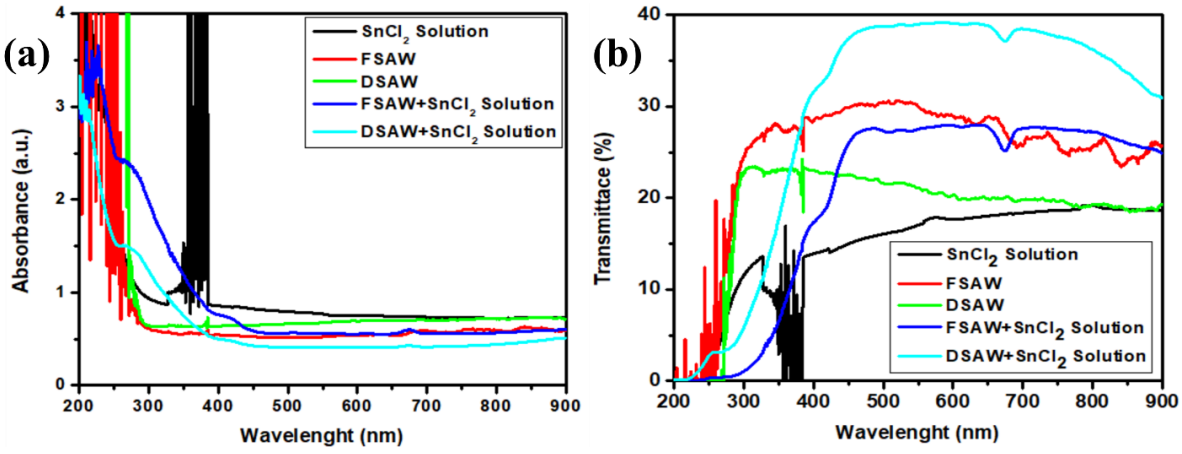

Figures 6: Absorbance-wavelength and Transmittance-wavelength plots of synthesized SnO_2 nanoparticles extracted $SnCl_2$, FSAW, DSAW, FSAW+$SnCl_2$ and DSAW+$SnCl_2$

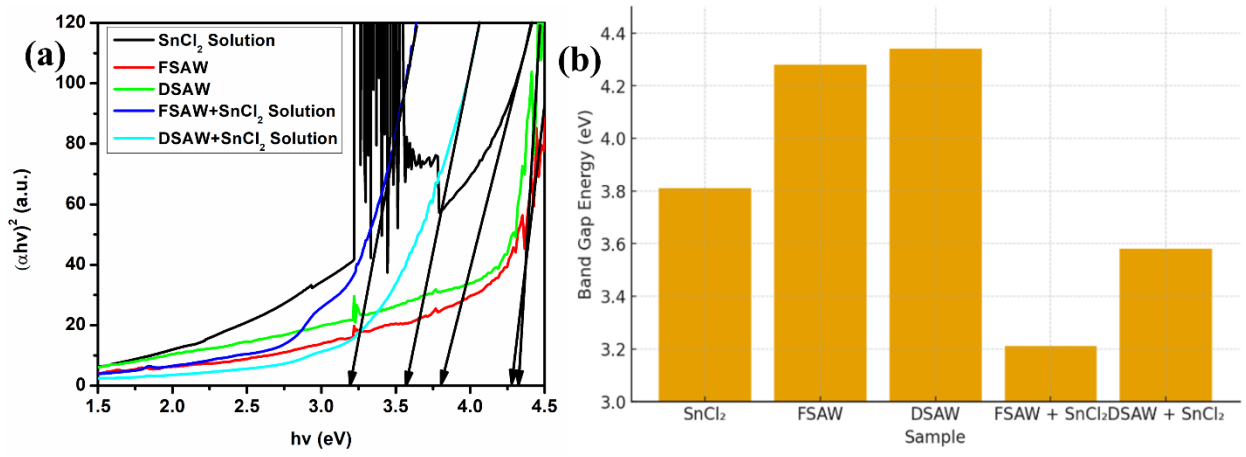

Figures 7: Absorption coefficient-energy gap plots and variation of optical band gap of synthesized SnO_2 nanoparticles extracted: $SnCl_2$, FSAW, DSAW, FSAW+$SnCl_2$ and DSAW+$SnCl_2$.

The thermal conductivity varied significantly with changes in the leaf extraction condition (fresh versus dry), directly influencing the suitability and applicability of the nanoparticles for specific temperature-dependent technological applications (Yasmin *et al*., 2023, Goswami *et al*., 2025). At lower temperatures (50°C and 100°C), the higher thermal conductivity values were observed in Sample FSAW+$SnCl_2$, which was synthesized using fresh leaves with an aqueous solvent, achieving a thermal conductivity of 196.4 W/m·K at 50°C. This notably high initial thermal conductivity suggests excellent potential for specialized applications such as thermal interface materials (TIMs) in low-temperature electronics or devices where rapid heat dissipation is required during system startup or early operational phases (Sivarajan *et al*., 2025, Hao *et al*., 2023). The high thermal conductivity at lower temperatures implies enhanced phonon transport efficiency, likely arising from improved crystallinity, reduced defect density, or favourable surface properties imparted by the fresh leaf extract synthesis route (Sivarajan *et al*., 2025).

As the temperature increased to 170°C, most samples experienced a systematic decline in thermal conductivity, a behaviour commonly attributed to increased phonon-phonon Umklapp scattering that reduces heat transport at elevated temperatures (Goswami *et al*., 2025, Yasmin *et al*., 2023). This temperature-dependent decline is consistent with known phonon transport phenomena in semiconductor nanostructures, where phonon mean free paths are shortened with increasing temperature, leading to lower thermal conductivity (Goswami *et al*., 2025).

At higher temperatures (250°C and 300°C), The two samples continued to show a gradual decrease in thermal conductivity, consistent with intensified phonon scattering dominating heat transport in nanomaterials at elevated temperatures (Goswami *et al*., 2025; Yasmin *et al*., 2023; Ouyang *et al*., 2025). Despite this reduction, the thermal conductivity values remained relatively high, particularly in Sample FSAW+$SnCl_2$, which maintained values of 156.4 W/m·K at 250°C and 150.4 W/m·K at 300°C. These findings support the use of biologically synthesized SnO_2 nanoparticles for demanding high-temperature thermal management applications, including power electronics and solar energy systems, where retention of substantial thermal conductivity is critical (Yasmin *et al.,* 2023; Goswami *et al.,* 2025).

Overall, this investigation demonstrates that careful selection of the biological condition of plant leaves used in the green synthesis process enables

systematic tuning of the thermal transport properties of SnO_2 nanoparticles. Samples synthesized using fresh leaves with aqueous solvent are particularly suitable for applications requiring stable and sustained thermal conductivity over low to moderately high temperature ranges (Yasmin et al., 2023, Sivarajan *et al.,* 2025).

Table 4: Thermal conductivities of the Synthesized SnO_2 Nanoparticles FSAW+$SnCl_2$ and DSAW+$SnCl_2$ measured in W/mK

Sample	Leaf Type	Solvent	50 °C	100 °C	170 °C	200 °C	250 °C	300 °C
FSAW+$SnCl_2$	Fresh	Water	196.4	186.5	188.4	155.2	156.4	150.4
DSAW+$SnCl_2$	Dry	Water	192.5	182.4	122.3	154.6	142.3	143.2

CONCLUSION

This study clearly demonstrated that the influence of plant material condition (fresh versus dried *Senna alata* leaves) plays a decisive role in governing the structural, morphological, optical, and thermal properties of biosynthesized SnO_2 nanoparticles. Across all characterization techniques, nanoparticles synthesized using the fresh aqueous leaf extract (FSAW+$SnCl_2$) consistently exhibited superior performance compared to those obtained from the dried aqueous leaf extract (DSAW+$SnCl_2$).

XRD analysis confirmed the successful formation of phase-pure tetragonal rutile SnO_2 in both samples; however, the fresh-leaf route yielded significantly smaller crystallite sizes (3.7 nm) and higher peak sharpness, indicating improved crystallinity. This enhancement is attributed to the higher concentration and activity of phytochemicals such as flavonoids and phenolic compounds retained in the fresh leaves, which promoted faster nucleation and better control over crystal growth. In contrast, partial degradation of these bioactive compounds during drying resulted in larger crystallites (8.2 nm) and comparatively reduced crystallinity.

FTIR spectra further substantiated the influence of condition of leaf, revealing stronger and more distinct functional groups (O–H, C–H, C–O, and NO_3^-) in the fresh-extract-derived nanoparticles. These functional groups acted effectively as reducing and capping agents, enhancing surface passivation and nanoparticle stability. The reduced intensity and slight shifts observed in the dried-leaf sample reflect diminished organic interactions due to thermal and oxidative changes during leaf drying.

Morphological investigations (SEM and TEM) showed that both synthesis routes produced spherical, well-dispersed SnO_2 nanoparticles with minimal agglomeration. Nevertheless, the FSAW+$SnCl_2$ derived nanoparticles displayed improved surface uniformity and dispersion, consistent with stronger steric stabilization from fresh phytochemicals. EDX analysis confirmed high elemental purity for both samples, with dominant Sn and O signals and complete elimination of chlorine residues, validating the effectiveness of the green synthesis approach.

Optical studies further highlighted the advantages of fresh-leaf extract. The FSAW + $SnCl_2$ system exhibited higher absorbance, lower transmittance, and a narrower optical band gap (3.21 eV) compared to the dried-leaf counterpart (3.58 eV). These features indicate enhanced light–matter interaction, higher particle density, and improved electronic delocalization, making the fresh-extract-derived SnO_2 nanoparticles more potential for

photocatalysis, UV-shielding, optoelectronics, and gas-sensing applications.

Thermal conductivity measurements revealed that nanoparticles synthesized from fresh leaves possessed superior heat-transport capability, particularly at lower temperatures, due to better crystalline quality and reduced phonon scattering. Even at elevated temperatures, both samples maintained relatively high thermal conductivity, confirming their applicability in thermal management and high-temperature electronic systems**,** with fresh-leaf-derived nanoparticles offering broader operational advantages.

The results conclusively show that using fresh *Senna alata* leaf extract is more effective than dried extract for the green synthesis of SnO_2 nanoparticles**,** yielding smaller crystallite sizes, enhanced crystallinity, improved optical activity, and superior thermal performance. This work underscores the critical importance of condition of leaf extracts in plant-mediated nanoparticle synthesis and provides a practical strategy for tailoring SnO_2 nanoparticle properties for potential sustainable applications in energy, environmental remediation, sensing, and thermal management technologies.

REFERENCES

Abiodun A. J., Alamu G. A., Adedokun O., Daramola O. O., & Sanusi Y. K (2024b). Iron oxide green synthesized nanoparticles for improved performance in monolithic dye-sensitized solar cells. *LAUTECH Journal of Engineering and Technology 18 (2), 128-137.*

Abiodun, A. J., Alamu, G. A., Daramola, O. O., Adedokun, O., & Sanusi, Y. K. (2024a). Green Synthesis of Copper Oxide Nanoparticles for Improved Performance in Monolithic Dye-Sensitized Solar Cells. *Fountain Journal of Natural and Applied Sciences.* 13(2), 23 – 34.

Adedokun, O., Awodele, M. K., Sanusi, Y. K. & Awodugba, A.O. (2018). Natural dye extracts from fruit peels as sensitizers in ZnO-based dye-sensitized solar cells, IOP Conf. Ser. 173, 012040. https://doi.org/10.1088/1755-1315/173/1/012040

Alanazi, S., Alaizeri, Z. M., Lateef, R., Madkhali, N., Alharbi, A. & Ahamed, M. (2023). Zn Doping Improves the Anticancer Efficacy of SnO_2 Nanoparticles. *Applied Science,* 13(22), 12456. https://doi.org/10.3390/app132212456

Alzahrani, B., Elderdery, A. Y., Alzerwi, N. A. N., Alsrhani, A., Alsultan, A., Rayzah, M., Idrees, B., Rayzah, F., Baksh, Y., Alzahrani, A. M., Subbiah, S. K., & Mok, P. L. (2023). Pluronic-F-127- Passivated SnO_2 Nanoparticles Derived by Using *Polygonum cuspidatum* Root Extract: Synthesis, Characterization, and Anticancer Properties. *Plants 12*, 1760. https://doi.org/10.3390/plants12091760

Aondona, I. P., EdemEssien, G. & Thompson, O. S. (2018). Biosynthesis of Eco-Friendly Silver Nano-Particles: The Efficiency of Fresh Leaves and Dried Leaves in the Synthesis of Silver Nanoparticles. *International Journal of Trend in Scientific Research and Development (IJTSRD)*. 2(3), 1019-1031

Blessi, S., MariaLuminaSonia, M., Vijayalakshmi, S., & Pauline, S. (2014). Preparation and characterization of SnO2 nanoparticles by hydrothermal method. *Int. J. Chem. Res.*, *6*, 2153–2155.

Buniyamin, I., Halim, M. F. A., Eswar, K. A., Alani, K. J., Kadir, S. A. I. A. S. A., Mohammad, M., Idorus, M. Y., Asli, N. A., Mahmood, M. R., & Khusaimi, Z. (2023). Natural Biomolecules in Leaves and Fruit Extracts Mediate the Biosynthesis of SnO2 Nanoparticles: A Mini Review. International Journal of Pharmaceuticals, Nutraceuticals and Cosmetic Science, 6(2), 24-40, https://doi.org/10.24191/ijpnacs.v6i2.03

Chaitra, C., Kalpana, H., Ananda, C., & Lalithamba, H. S. (2023). Dielectric properties of green synthesized Sb:SnO_2 nanoparticles. In 2023 International Conference on Smart Systems for applications in Electrical Sciences (pp. 1-5). IEEE. https://doi.org/10.1109/ICSSES58299.2023.10201159

Chen, X., Huang, B., Zhang, C., Li, P., & Wang, P. (2017). Tunable SnO_2 Nanoribbon by Electric Fields and Hydrogen Passivation. *Journal of Nanomaterial,* 2017, 1–12.

Din, S.U., Kiani, S.H,. Haq, S., Ahmad, P., Khandaker, M.U., Faruque, M.R.I., Idris, A.M., & Sayyed, M.I. (2022). Bio-Synthesized Tin Oxide Nanoparticles: Structural, Optical, and Biological Studies. Crystals, *12*(5), 614; https://doi.org/10.3390/cryst12050614

Goswami, Y. C., Bisauriya, R., Goswami, R., Hlaing, A. A., &Moe, T. T. (2025). Hydrothermal synthesis of SnO_2/cellulose nanocomposites: optical, structural, and morphological characterization. *Scientific Reports*, 15**,** 9752. https://doi.org/10.1038/s41598-025-87948- y

Hao, N. V., Tung, D. H., Thao, T. T. Hoa, V. X., Thoan, N. H., Tan, P. T., Minh, P. N., Fal, J., Zyla, G., & Trinh, P. V. (2023). High thermal conductivity of green nanofluid containing Ag nanoparticles prepared using plant extract. *Journal of Thermal Analysis and Calorimetry*, 148**,** 7579–7590. https://doi.org/10.1007/s10973-023-12266-2

Haq, S., Ehsan, R., Menaa, F., Shahzad, N., Din, S. U., Shahzad, M. I., Rehman, W., Waseem, M., Alrhabi, W., Almukhlifi, H. A., & Alsharef, S. A. (2022). A Novel Shift in the Absorbance Maxima of Methyl Orange with Calcination Temperature of Green Tin Dioxide Nanoparticle- Induced Photocatalytic Activity. *Catalysts*, *12*(11), 1397; https://doi.org/10.3390/catal12111397

Hariprasad, H., Bai, G. S., Santhoshkumar, J., Madhu, C. H., Sravani, D. (2016). Green Synthesis of Copper Nanoparticles by Arevalanata Leaves Extract and their AntiMicrobial Activites. *International Journal of ChemTech Research*. 9(2), 98-105.

Karmaoui, M., Jorge, A. B., McMillan, P., Aliev, A., Pullar, R., Labrincha, J., & Tobaldi, D. (2018). One-step synthesis, structure, and band gap properties of SnO_2 nanoparticles made by a low temperature nonaqueous sol–gel technique. *ACS Omega*, 3(10), 13227-13238. https://doi.org/10.1021/acsomega.8b02122

Kaur, M., Prasher, D., & Sharma, R. (2023). Influence of heat treatment on the properties of tin oxide nanoparticles: A potential material for environmental remediation applications. *Environment Conservation Journal*, 24(2), 164-172. https://doi.org/10.36953/ecj.16482524

Letifi, H., Dridi, D., Litaiem, Y., Ammar, S., Dimassi, W., & Chtourou, R. (2021). High Efficient and Cost Effective Titanium Doped Tin Dioxide Based Photocatalysts Synthesized via Co-precipitation Approach. *Catalysts, 11*(7),803; https://dpi.org/10.3390/catal11070803

Lithi, I. J., Nakib, K. I. A., Chowdhury, S. A. M., & Hossain, M. (2025). A review on the green synthesis of metal (Ag, Cu, and Au) and metal oxide (ZnO, MgO, Co_3O_4, and TiO_2) nanoparticles using plant extracts for developing antimicrobial properties. *Nanoscale Advances*, 7, 2446-2473.https://doi.org/10.1039/d5na00037h

Matussin, S. N., Harunsani, M. H., Tan, A. L. & Khan, M. M. (2020). Plant-extract-mediated SnO_2 nanoparticles: Synthesis and Applications. *ACS Sustainable Chemistry & Engineering*, *8*(8),3040–3054. https://doi.org/10.1021/acssuschemeng.9b06398

Narasaiah, B. P., Banoth, O., Sohan, A., Mandal, B., Bustamante Dominquez, A. B., de los Santos Valladare, L., & Kollu, P. (2022). Green biosynthesis of tin oxide nanomaterials mediated by agro-wast cotton boll peel extracts for the remediation of environmental pollutant dyes. *ACS Omega*, 7, 15423-15438. https://doi.org/10.1021/acsomega.1c07099

Narayanan, N. (2012). Synthesis of green nano catalysts and industrially important green reactions. *Green Chemistry Letters and Reviews.* 5(4), 707-725.

Ouyang, N., Shen, D., Wang, C., Cheng, R., Wang, Q., & Chen, Y. (2025). Positive temperature-dependent thermal conductivity induced by wavelike phonons in complex Ag-based argyrodites. *Physical Review B,* 111(6), 064307. https://doi.org/10.1103/physrevb.111.064307

Rahim, N. A., Ferdosh, S., Zainuddin, N. A. N. B., & Sarker, M. (2022). Extraction methodologies, phytochemical constituents and biological activities of *Senna alata* Linn: A review. *The Natural Product Journal*, 12(2), 114719.

Saravanakumar, M., Agilan, S., Muthukumarasamy, N., Rukkumani, V., Marusamy, A., Umamaheshwari, P., & Ranjitha, A. (2014). Photoluminescence Studies on Nanocrystalline Pure and Cr Doped Tin Oxide Powder. *International Journal of ChemTech Research,* 6(14), 5429–5432.

Sarwar, K., Nazli, Z. H., Munir, H., Aslam, M. & Khalofah, A. (2025). Biosynthesis of zinc oxide nanoparticles using *Moringa oleifera* leaf extract, probing antibacterial and antioxidant activities *Scientific Reports*, *15*, 20413. https://doi.org/10.1038/s41598-025-08839-w

Singh, H., Desimone, M., Pandya, S. R., Jasani, S., George, N., Adnan, M., & Alderhami, S. A.(2023). Revisiting the green synthesis of nanoparticles: Uncovering influences of plant extracts as reducing agents for enhanced synthesis efficiency and its biomedical applications. *International Journal of Nanomedicine*, 18, 4727-4750. https://doi.org/10.2147/IJN.S419369

Sivarajan, Y., Ishak, K. A., & Yaacob, J. S. (2025). Green Synthesis of Tin Oxide (SnO_2) Nanoparticles Using Ginger Extracts for Photocatalytic Degradation of Organic Dyes in Wastewater. *Applied Biochemistry and Biotechnology*, *197*, 5668–5693. https://doi.org/10.1007/s12010-025-05293-2

Toloman, D., Popa, A., Raita, O., Stan, M., Suciu, R., Miclaus, M.O., & Biris, A.R. (2014). Luminescent properties of vanadium-doped SnO_2 nanoparticles. *Opt. Mater.*, *37*, 223–228.

Villagrán, Z., Anaya-Esparza, L. M., Velzquez-Carriles, C., Silva-Jara, J., Ruvalcaba-Gmez, J. Aurora-Vigo, E. F., ... & Martínez-Esquivias, F. (2024). Plant-based extracts as reducing, capping, and stabilizing agents for the green synthesis of inorganic nanoparticles. *Resources*, 13(6), 70. https://doi.org/10.339f0/resources13060070

Yagi, S., Cetiz, M. V., Zengin, G., Bakar, K., Himidi, A. A., Mohamed, A., & Gai, U. (2024). Novel natural candidates for replacing synthetic additives in nutraceutical and pharmaceutical areas: Two Senna species (*S. alata* (L.) Roxb. and *S. occidentalis* (L.) Link). *Food Science & Nutrition*, 13(5), 4705. https://doi.org/10.1002/fsn3.4705

Yasmin, H., Giwa, S. O., Noor, S., & Sharifpur, M. (2023). Thermal Conductivity Enhancement of Metal Oxide Nanofluids: A Critical Review. *Nanomaterials*, 13(3), 597. https://doi.org/10.3390/nano13030597